Mechanistic model of an oil-flooded single-screw expander

Davide ZIVIANI[1*], Ian H. BELL[2], Michel DE PAEPE[1], Martijn VAN DEN BROEK[1]

[1] Ghent University, Department of Flow, Heat and Combustion Mechanics,
Kortrijk, Belgium
[2] University of Liège, Thermodynamics Laboratory,
Liège, Belgium
Contact Information: Davide.Ziviani@UGent.be

* Corresponding Author

ABSTRACT

The power generated from Organic Rankine Cycles (ORCs) is directly related to the performance of the expander used, which in many cases it is adapted from the original compressor. The efficiency of positive displacement expanders depends on several aspects such as internal volume ratio and pressure ratio (under- and over-expansion), leakages, non-adiabatic expansion and heat losses to the ambient and mechanical losses. Thus, lubrication is often required to reduce friction and to seal leakage gaps. In this paper, the effect of oil-flooding on the performance of a single-screw expander is investigated. By varying the oil fraction, it is possible to analyze the combined effects of reducing the leakages and the possibility to achieve a quasi-isothermal expansion. The flooding of the expander is realized by adding an independent oil loop to the conventional ORC as proposed by Woodland et al. (2013). The mechanistic model developed by Ziviani et al. (2014) for a single-screw expander has been extended to include liquid-flooding. The multi-chamber model with the associated governing equations of conservation of mass and energy for the flooded-expansion process is described along with the overall energy balance model of the expander. Insights on the calculation of the working fluid and lubricant oil mixture properties and the solubility effects are provided. The working fluid considered is R245fa and the lubricant oil is ACD100FY. The mechanistic model is implemented in the Python programming language and the oil-flooded single-screw expander model is integrated in the open-source simulation package PDSim (v3.0).

1. INTRODUCTION

The performance of an organic Rankine cycle depends on the operating conditions of the heat source and cold sink, on the selection of the working fluid to exploit the heat source and on the selection and sizing of the expander. During the last decades, the research on positive displacement machines as expanders for ORC systems is intensified. A comprehensive review of volumetric expanders for low grade heat recovery has been published by Imran et al. (2016). A comparative assessment showed that scroll and screw expanders achieved the highest scores because of the balance between internal losses (mainly leakage and friction losses) and overall performance.

In order to optimize the work extraction for waste heat, different cycle architectures can be investigated Lecompte et al. (2015). As shown by Woodland et al. (2014), ORC with flash expansion from saturated liquid or from a two-phase mixture with a low vapor quality presented a higher Second Law efficiency compared to baseline ORC with a net increase of power conversion percentage of the heat source exergy rate.

Theoretically, the expansion process can also be improved by moving the expansion work path from an adiabatic process toward an isothermal process (Igobo & Davies, 2014). In an organic Rankine cycle, a quasi-isothermal process can be achieved by flooding the expander with a secondary fluid (typically oil) which acts as thermal buffer. Such concept was analyzed by Woodland et al. (2013) and Georges (2012). The scroll expander used had a small internal volume ratio (< 2) which limited the benefits of the flooding process with respect to the effective internal volume ratio. It was suggested that an expander with a larger volume ratio, such as screw-type, could be more suitable.

In this paper a single-screw expander is considered to investigate the benefits of an oil-flooded expansion. A generalized chamber model needs to be developed to improve existing models in the literature to be able to describe any expansion (or compression) processes including flashing and two-phase expansion, oil-flooded, oil-injected, etc.

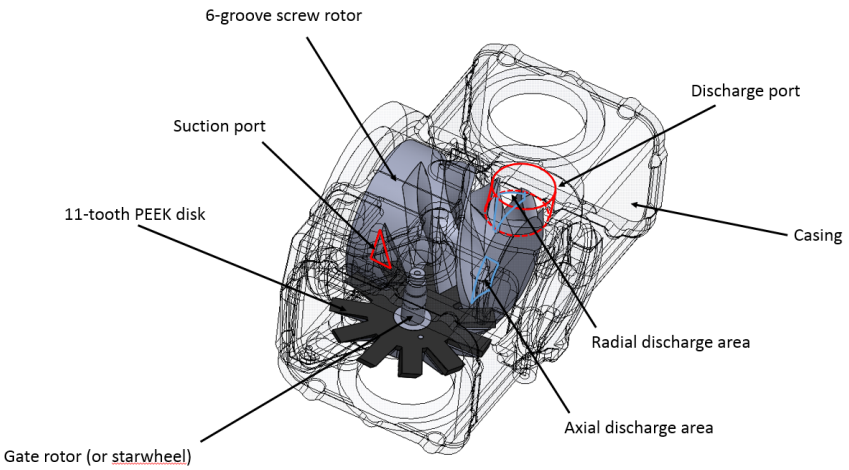

Figure 1: 3D CAD model of the single-screw expander considered in the present work with the different control volumes indicated.

2. SINGLE-SCREW GEOMETRY MODEL

The single-screw expander considered in this work is an oil-injected 11 kW air-compressor adapted to perform as expander. The main geometric characteristics are listed in Table 1. Furthermore, the complete formulation of the geometry model can be found in Ziviani et al. (2014) and Ziviani et al. (2015). In the following subsections, the main improvements on the geometry model are briefly described.

2.1 Extension of the compressor model

The expander model proposed in Ziviani et al. (2014) was derived from the well-known compressor model established by Bein and Hamilton (1982). The expansion process was considered to occur identically in both sides of the rotor which simplified the overall model. The model is extended here to undertake a more comprehensive description of the machine. The single-screw expander and the definition of different control volumes are shown in Figure 1. In particular, both sides of the expander are modeled which allows to a better estimation of the suction losses and to more accurate model of the discharge process as expander. In fact, in the current expander the main housing outlet port is located on one side which means that the effective discharge area is different in the two sides of the expander. As a consequence the volume of the groove needs to be predicted throughout one rotation.

2.2 Volume Curve and Port Sizes

The calculation of the chamber volumes and the porting are done by describing the single-screw geometry by means of polygons, i.e. arrays of node coordinates. Polygon operations are employed to obtain intersections and through Green's theorem areas and volumes are computed, as described in Bein and Hamilton (1982) and Ziviani et al. (2015). While the single-screw compressor models reported in literature start at the end of suction process (beginning of discharge in the case of expander), in the present model, the groove return volume curve is also important to describe the discharge process. The polygon model of the single-screw geometry is shown in Fig. 2. The intersection operation between the starwheels and the main rotor is shaded in grey. At each rotation angle and for each tooth engaged, the area, A_i, and the position of the centroid (c_z, c_r) are calculated and the volume of the groove is obtained as:

$$V(\theta) = \sum_i c_r A_i \Delta\theta \tag{1}$$

The decrease of groove volume after around 180°of rotation is done by subtracting the volume of the expansion chamber increasing on the other side of the rotor. Similar approach is also used to calculate the groove surface.

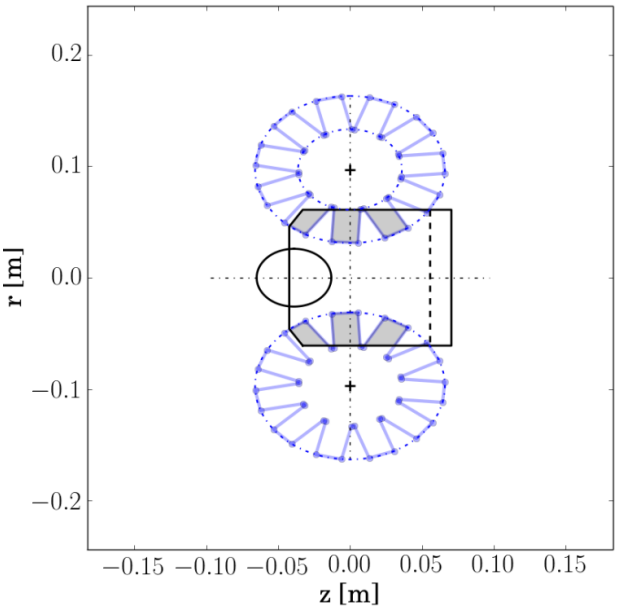

Figure 2: Polygon clipping applied to single-screw expander geometry.

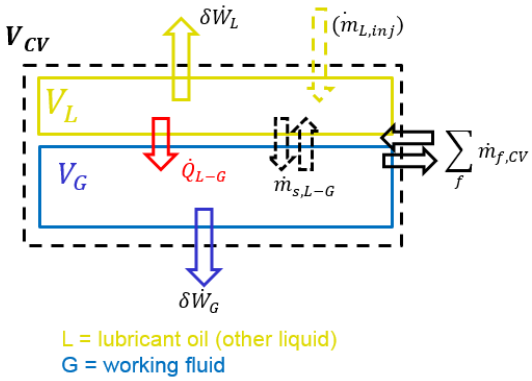

Figure 3: General schematic of a control volume.

The area of suction and discharge ports with respect the crank angle are determined in a similar fashion. The main rotor and the groove are unwrapped and the intersection between the groove with the triangular suction port is obtained through polygon intersection. On both sides of the rotor, the axial discharge port defined by the shape of the end of the groove is the same. As previously mentioned, only on the side with the main outlet of the housing, the groove presents a radial discharge area. By unwrapping the groove, the length of leading and trailing edges can be determined at each crank angle (Ziviani et al., 2015).

3. THERMODYNAMIC MODEL

Different thermodynamic models have been considered in literature to analyze oil-flooded compressors. In particular, Fujiwara et al. (1984) developed an oil-flooded screw compressor model by applying the conservation of mass and energy of an open control volume to both the working fluid and oil. The heat exchange between the working fluid and the oil was also taken into account with a term proportional to the temperature difference between the two fluids. However, the working fluid was treated as an ideal gas and could not change phase. An improvement of such model was done by Stosic et al. (1988) by describing the oil-injection process in details including the influence of the oil droplet size. A significant contribution on handling large amount of liquid in the working chamber was proposed by Bell et al. (2012). In particular, the lubricant oil and the working fluid were considered as a homogeneous mixture and the oil-flooded compressor and expander were modeled by solving the governing equations of conservation of mass of working fluid, oil mass fraction and energy for each working chamber.

Regarding two-phase expansion, Taniguchi et al. (1988) proposed thermodynamic model of a two-phase working fluid in screw expanders by applying conservation of mass and energy to different phases of the expansion process. The specific volume, internal energy and quality were chosen as state variables. The presence of lubricant oil was not taken into consideration. A similar approach was also adopted by Smith et al. (1996) to carry out an extensive study on two-phase expansion in screw machines.

Specifically to single-screw compressor, Wu and Jin (1988) developed a simulation model which accounted for the impact of oil injected into the working chamber and the effects on the leakages. The heat transfer between oil and working fluid was neglected and the working fluid was treated as ideal gas with no phase change. Shear power losses due to the presence of oil were taken into account. A mechanical analysis on the forces and torques was not considered.

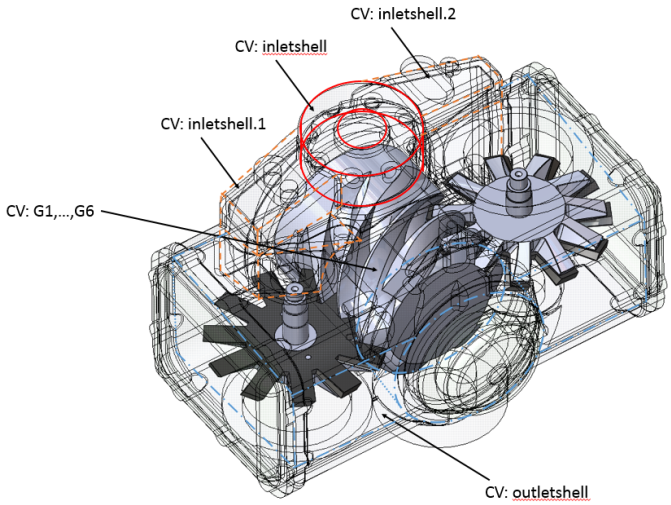

Figure 4: Definition of the different control volumes in a single-screw expander.

A more generalized chamber model is required to model:

- oil-flooded compressors/expanders (two-fluid model);
- phase change of working fluid (flash or two-phase expansion). Compressor slugging can also be modeled;
- allow for liquid/vapor/two-phase injections;
- account for heat transfer between phases when the assumption of thermal equilibrium is not valid (e.g. isothermal expansion);
- working fluid and lubricant oil can leak independently or as mixture.

3.1 Definition of a General Geometric Control Volume

In order to establish a set of governing equations, the structure of a general control volume (CV) needs to be defined. By referring to Figure 3, a general CV, which corresponds to the actual geometry of the working chamber, is divided into two part: working fluid (G) and lubricant oil or other flooding mediums (L). According to Ishii and Hibiki (2011), for a two-fluid model the volume occupied by each fluid can be estimated by introducing the void fraction α:

$$\alpha = \frac{1}{1 + \frac{x_L}{1-x_L} S \frac{v_L}{v_G}} \tag{2}$$

$$V_{CV} = \alpha V_{CV} + (1-\alpha) V_{CV} = V_G + V_L \tag{3}$$

where S is the slip ratio. A slip model between the fluids can be introduced which requires the calculation of the fluid velocities. At first, the slip ratio is assumed unity (mechanical equilibrium). A simplified version of Equation 3 was

Table 1: List of geometric parameters of the single-screw expander.

Parameter	Value
Engaging ratio [-]	11/6
D_{sr} [mm]	122
D_{sw} [mm]	132
$V_{g,max}$ [cm^3]	57.39
$r_{v,built-in}$ [-]	5.3
L_{rotor} [m]	121

adopted by Mathison et al. (2013), where the working fluid volume was estimated by subtracting the volume of oil to the total chamber volume.

The governing equations of conservation of mass and energy are applied to each fluid. In a complete two-fluid model, also the momentum equations should be included. The CVs of identified in a single-screw expander are shown in Figure 4 and they can be distinguished between stationary (inlet and outlet shell CVs) and rotating CVs (grooves G1,...,G6).

3.2 Extension of the Chamber Model

To establish the two-fluid model, a set of differential equations need to be derived. The following assumptions are made:

- the working fluid (G) can change phase and the saturated vapor and liquid phases are denoted as *g* and *l*, respectively;
- working fluid and lubricant oil are treated as separate fluids. Oil-refrigerant interaction occurs through heat transfer and mass transfer (solubility effect). The flashing of oil is neglected;
- working fluid and oil thermodynamic states are homogenous throughout the control volume at any moment;
- the kinetic and potential energy term are neglected. Therefore, the total energy of the control volume is $E_{CV} \simeq (mu)_{CV}$.

For each fluid, the conservation of mass and energy are applied. When the working fluid is has a superheated state, density and temperature, i.e. (ρ, T), are chosen as state variables. The rate of change of the working fluid mass in the control volume can be conveniently written as:

$$\rho_G \frac{dV_G}{d\theta} + V_G \frac{d\rho_G}{d\theta} = \frac{1}{\omega}\left[\sum_i \dot{m}_{G,i} \pm (..)\right] \tag{4}$$

Analogously for the secondary liquid phase:

$$\rho_L \frac{dV_L}{d\theta} + V_L \frac{d\rho_L}{d\theta} = \frac{1}{\omega}\left[\sum_i \dot{m}_{L,i} \pm (..)\right] \tag{5}$$

In the RHS of the above equations, additional terms may include working fluid dissolved in the oil or oil vapor in the working fluid. If the secondary liquid phase is expressed as a fraction of the working fluid, Equation 5 can be reworked as proposed by Bell et al. (2012).

The conservation of energy for the two phases is given by:

$$\frac{d(mu)_G}{d\theta} = \frac{1}{\omega}\left[\sum \dot{Q}_{G,b} + \sum_i \dot{m}_{G,i} h_{G,i} + \sum \dot{W}_{G,b} + \dot{Q}_{L-G}\right] \tag{6}$$

$$\frac{d(mu)_L}{d\theta} = \frac{1}{\omega}\left[\sum \dot{Q}_{L,b} + \sum \dot{Q}_{L,mt} + \sum \dot{W}_{L,b} + \sum \dot{W}_{L,mt} - \dot{Q}_{L-G}\right] \tag{7}$$

where:

- $\dot{Q}_b$: heat transfer rate through the boundary of the control volume
- $\dot{Q}_{mt}$: heat transfer rate to the control volume by mass transfer
- $\dot{W}_b$: work rate through the boundary of the control volume
- $\dot{W}_{mt}$: work rate to the control volume by mass transfer
- $\dot{Q}_{L-G}$: heat transfer rate between the two phases.

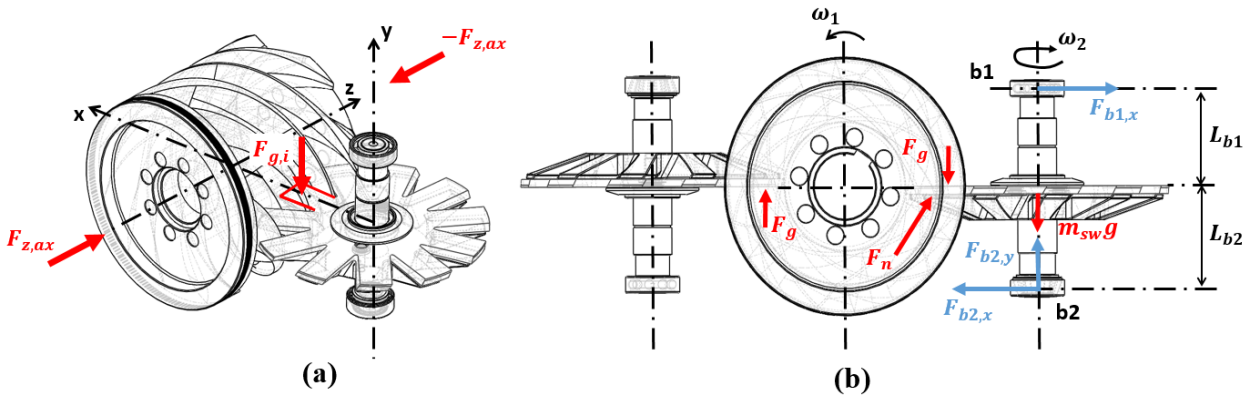

Figure 5: Forces and torques balance on the starwheel.

By reworking Equation 6 and Equation 7, the expressions for $dT_G/d\theta$ and $dT_L/d\theta$ can be obtained.

When the working fluid condition in the control volume is two-phase, temperature and quality need to be considered along with the density in order to accurately define a thermodynamic state. The specific enthalpy of the working fluid is then given by:

$$h_G = x_g h_{G,g} + (1 - x_g) h_{G,l} \tag{8}$$

where the saturated properties are only functions of temperature. By differentiating the specific enthalpy with respect temperature and quality:

$$\frac{dh_G}{d\theta} = \left(\frac{\partial h_G}{\partial T}\right)_{x_g} \frac{dT}{d\theta} + \left(\frac{\partial h_G}{\partial x}\right)_T \frac{dx_g}{d\theta} = \left[x_g \frac{dh_g}{dT} + (1 - x_g)\frac{dh_l}{dT}\right]\frac{dT}{d\theta} + (h_g - h_l)\frac{dx_g}{d\theta} \tag{9}$$

Therefore, the derivative of the specific internal energy becomes:

$$\frac{du_G}{d\theta} = \left[x_g \frac{dh_g}{dT} + (1 - x_g)\frac{dh_l}{dT}\right]\frac{dT}{d\theta} + (h_g - h_l)\frac{dx_g}{d\theta} - \frac{p(\theta)}{m_G}\frac{dV_G}{d\theta} + \frac{pV_G}{m_G^2}\frac{dm_G}{d\theta} \tag{10}$$

By recalling that the specific volume of the two-phase working fluid is equal to the volume to mass ratio of the working fluid, or:

$$x_g v_g + (1 - x_g) v_l = \frac{V_G}{m_G} \tag{11}$$

and by differentiating each side with respect the crank angle θ, the derivative of the quality with respect the crank angle, $dx_g/d\theta$, can be obtained:

$$\frac{dx_g}{d\theta} = \frac{1}{v_{G,g} - v_{G,l}}\left\{\frac{1}{m_G}\frac{dV_G}{d\theta} - \frac{V_G}{m_G^2}\frac{dm_G}{d\theta} - \left[x_g \frac{dv_{G,g}}{dT} + (1 - x_g)\frac{dv_{G,l}}{dT}\right]\frac{dT_G}{d\theta}\right\} \tag{12}$$

Last, the expression of the derivative of the specific energy with respect the crank angle:

$$\frac{du_G}{d\theta} = \left[x_g \frac{dh_{G,g}}{dT} + (1 - x_g)\frac{dh_{G,l}}{dT} - v_{G,g}\frac{dp}{dT}\Big|_{sat}\right]\frac{dT_G}{d\theta} + (h_{G,g} - h_{G,l})\frac{dx_g}{d\theta} - \frac{p(\theta)}{m_G}\frac{dV_G}{d\theta} + \frac{pV}{m_G^2}\frac{dm_G}{d\theta} \tag{13}$$

can be solved for $dT_G/d\theta$. The derived set of differential equations are integrated simultaneously by using an adaptive Runge-Kutta 4th/5th order solver. The thermo-physical properties of the working fluids are retrieved from CoolProp (Bell et al., 2014). Furthermore, the first saturation derivatives necessary in the case of two-phase conditions are also obtained from the low-level interface available within CoolProp. A library of lubricant oil has been created taking advantage of the CoolProp *State* class. The properties of ACD100FY are also available in Zhelezny et al. (2007).

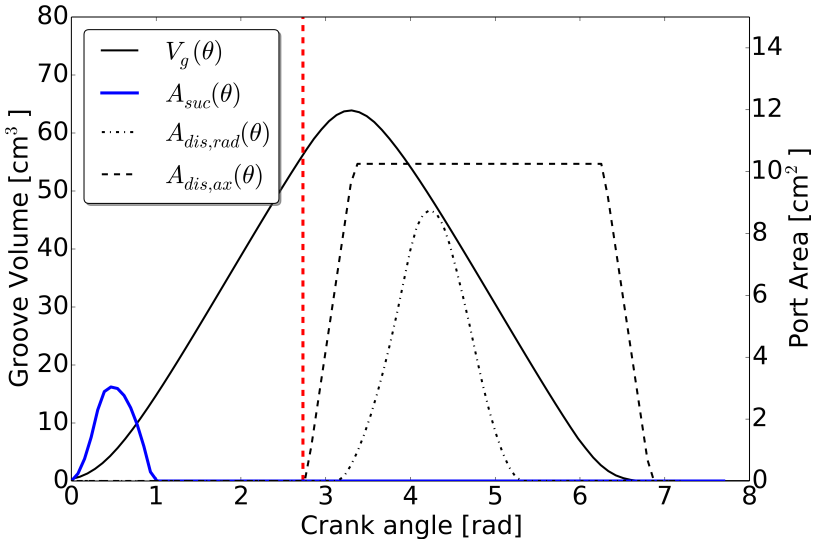

Figure 6: Variation of the groove volume with the crank angle. On the same plot, also the suction port and both radial and axial discharge ports as function of the crank angle are overlaid.

3.3 Overall Energy Balance

The expander model is closed by an overall energy balance applied to the expander shell. A lumped thermal mass model is adopted. The overall energy balance includes the heat fluxes interacting with the shell, the heat transfer loss to the ambient and the mechanical losses. The temperature of the lumped mass, T_{shell}, is obtained by minimizing the energy balance given by:

$$\dot{W}_{mech,loss} + \sum_i \left[\dot{Q}(T_{shell})\right] = 0 \tag{14}$$

In Ziviani et al. (2014), the mechanical losses were expressed by considering a friction torque τ_{loss}. In the present work, a mechanistic model for the mechanical losses is included. In particular, the loads on the starwheel and friction losses between starwheel and main rotor are considered. A schematic of forces on main rotor and starwheels is shown in Figure 5. Once the pressure trace in the working chambers is known at the end of one cycle, the force on each tooth generated by the expansion process is given by:

$$F_{g,i}(\theta) = p_i(\theta)A_i(\theta) \tag{15}$$

and it is applied on the centroid of the intersection tooth area (see Figure 2). As there are three tooth on each side constantly engaged, the total force due pressure loads is given by summing up each contribution, i.e. $\sum_i F_{g,i}, i = 1,2,3$.

The groove applies a force F_n which is perpendicular to the groove surface itself and direct to the tooth flank. As a consequence, F_n changes orientation with the helix angle of the groove during the expansion process. For each tooth, a frictional force component of $F_{n,i}$ can be obtained as:

$$F_{f,i} = \mu_g F_{n,i} \tag{16}$$

where the friction coefficient μ_g depends on the materials of groove and tooth and the presence of oil. The axial and radial force balances on the starwheel are given by:

$$F_{b2,y} - m_{sw}g - F_g + F_{n,y} = 0 \tag{17}$$

$$-F_{b1,x} - F_{n,x} + F_{b2,x} = 0 \tag{18}$$

where m_{sw} is the total mass of the starwheel body plus the toothed PEEK disk. By means of a balance of moments around the upper bearing, the loads on each bearing can be determined and the friction power can also be estimated through the thrust bearing theory.

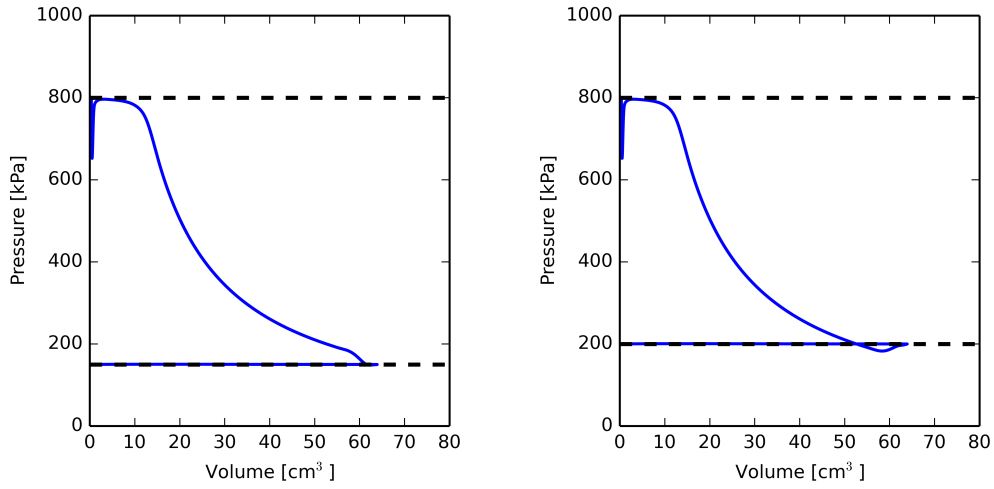

Figure 7: Pressure versus groove volume of single-screw expander (p_{su}= 800 kPa, T_{su}= 100 °C, x_L = 0.01, N = 3000 rpm): (a) under-expansion (p_{ex}= 150 kPa); (b) over-expansion (p_{ex}= 200 kPa).

4. RESULTS AND DISCUSSION

The complete groove volume curve and the port areas as function of the crank angle are shown in Figure 6. The ability of the geometry model to include also the return part of the groove volume while it starts wrapping on the opposite side of the rotor is important to simulate the under- and over- expansion as well as to quantify the flow losses during the discharge process. In Figure 7, the model has been exercised to obtain the p-V diagrams in both cases of under- and over-expansion. In particular, the inlet pressure and temperature are fixed at 800 kPa and 100 °C, the rotational speed of the main rotor is 3000 rpm and lubricant oil mass fraction is 0.01. Two values of the discharge pressure have been considered: 150 kPa (case with under-expansion) and 200 kPa (case with over-expansion). These values are also representative of the experimental operating conditions (Ziviani et al., 2015). By comparing the two p-V diagrams, it can be noted that the over-expansion, shown in Figure 7(b), is particularly detrimental for the performance of the machine with respect to under-expansion. Under the specified conditions, the slight over-expansion caused a 17% decreased in power output. Due to the fact that the internal volume ratio of the expander is around 5.3, the peak of isentropic efficiency was obtained for an applied pressure ratio between 6 and 8. The gas forces applied to each tooth during one full rotation are shown in Figure 8. The peak of force occurs at the end of the suction process.

The extended chamber model described in Subsection 3.2 has been tested by considering a two-phase expansion of R245fa and lubricant oil ACD100FY. The expander inlet conditions were specified in terms of temperature and quality, 100 °C and 0.6. The lubricant oil mass fraction was set to 0.05. The results of the two-phase expansion are shown in Figure 9. At each step size taken by the solver, the quality of the working fluid is updated by considering the actual volume occupied by the working fluid and its mass:

$$x_g = \frac{\frac{V_G}{m_G} - v_{G,l}}{v_{G,g} - v_{G,l}} \tag{19}$$

If $x_g < 0$ or $x_g > 1$, the working fluid is considered subcooled or superheated, respectively. Once x_g is calculated, its derivative $dx_g/d\theta$ can be evaluated. The evolution of pressure and quality with respect of the crank angle are reported in the top-left chart of Figure 9. During the expansion process, the quality of R245fa increases from 0.60 to 0.87 which corresponds to a specific volume ratio of approximately 17. Thus, the majority of the quality change occurs during the filling process and at the beginning of the closed expansion. As a result, the built-in volume ratio of the machine needs to be lower than the expansion volume ratio to avoid over-expansion and other internal losses. In the case of twin-screw machines, Smith et al. (1996) reported that the built-in volume ratio should be around 20-30% of

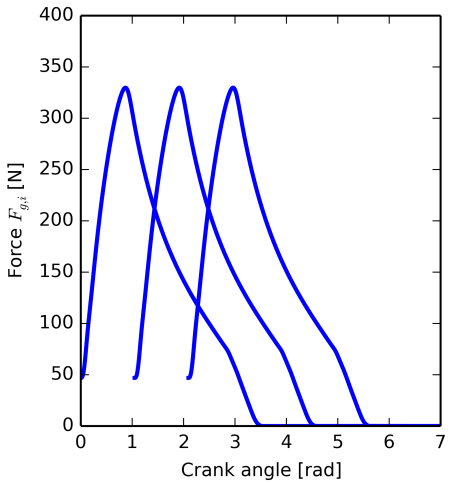

Figure 8: Force induced from the pressure inside the grooves on each tooth engaged during a rotation of the main rotor (p_{su}= 800 kPa, T_{su}= 100 °C, p_{ex}= 200 kPa, x_L = 0.01, N = 3000 rpm).

the overall expansion volume ratio. Under the considered two-phase expansion conditions, shown in the T-s diagram (top-right chart of Figure 9), the built-in volume ratio of the single-screw expander should be between 3.4 and 5.1. This result is in line with the geometry of the existing expander showing potential to explore two-phase expansion and partial-evaporating ORC.

The chamber model has the ability to estimate the temperature evolution of both working fluid and lubricant oil. Different models of heat transfer term $\dot{Q}_{L-G}$ can be applied depending on the data availability, oil-injection parameters etc. (Stosic et al., 1988) . In this case, the oil is pre-mixed with the working fluid prior entering the expander by means of a static mixer. Ideally, the static mixer creates an homogeneous fluid structure and therefore it is reasonable to assume an average oil droplet size to estimate the heat transfer. The heat transfer coefficient at the oil droplet surface is given by:

$$h_{L-G} = \frac{k_L}{D_{d,L}} \left[2 + 0.6 Re_L^{0.6} Pr_L^{0.33} \right] \tag{20}$$

where k_L is the thermal conductivity of the oil, $D_{d,L}$ is mean oil droplet diameter, Re_L and Pr_L represents the Reynolds and Prandtl numbers for the oil. The thermal behaviors of the working fluid and the oil droplet are shown in Figure 9. The thermal inertia of the two fluid is different and the temperature drop experienced by the working fluid is significantly higher under the two-phase conditions. However, the expansion process in the single-screw is quite fast (pressure variations are in the order of 8-9 ms/cycle) and in order to account for phenomena such heat transfer between oil and working fluid as well as oil and the chamber walls, more accurate correlation should be develop based on experimental results. To this end, a dedicated ORC test-rig with independent lubricant oil loop and mixing section have been designed and constructed. The chamber model is general enough to account for primary and secondary thermal effects.

5. CONCLUSIONS

In this paper, a mechanistic model of an oil-flooded single-screw expander has been presented. The main achievements are:

- by describing the main rotor and the starwheels as polygons, boolean operations can be used to obtain the full volume curve of each groove; by unwrapping each groove the suction and discharge porting can be accurately calculated. In a single-screw expander only one side presents a radial groove opening beside the main outlet of the housing;
- a generalized two-fluid chamber model has been implemented which allows to the working fluid to change phase and to account for the presence of oil. The models account for the heat transfer between the fluids;

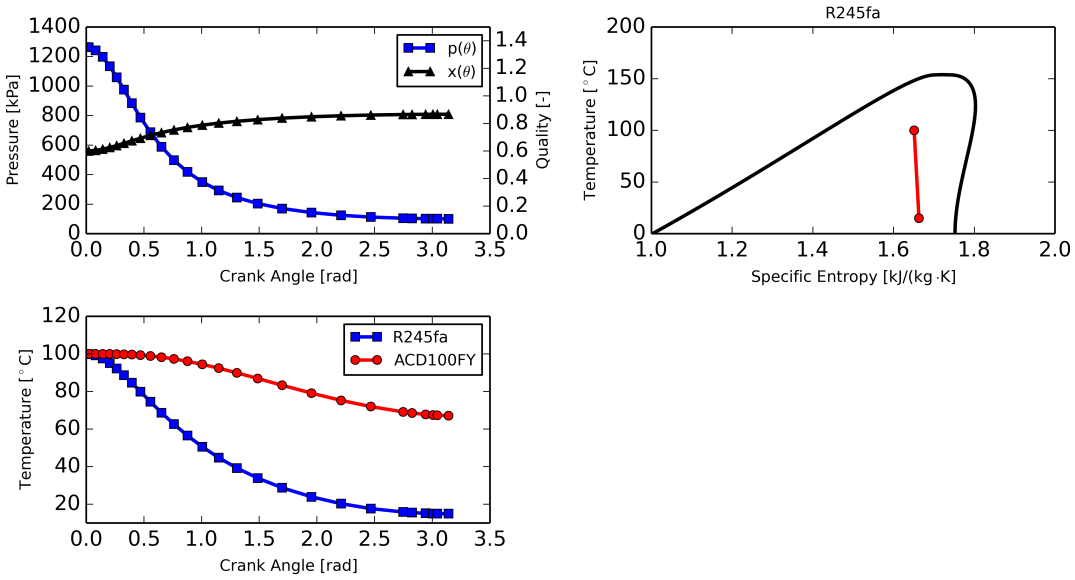

Figure 9: Example of two-phase expansion of R245fa with lubricant oil ACD100FY with the following boundary conditions: T_{su} = 100 °C, $x_{g,su}$=0.6, p_{ex} = 150 kPa, x_L = 0.05. The mean oil droplet size is 50 μm.

- a mechanistic models to compute the mechanical and friction losses on the starwheel has been added. Further work is required to estimate the mechanical torque generated at the main rotor shaft.

NOMENCLATURE

$\dot{m}$	mass flow rate	(kg/s)	**Subscript**	
c	centroid coordinates	(m)	CV	control volume
D	diameter	(m)	ex	exhaust
F	force	(N)	d	droplet
h	specific enthalpy	(kJ/kg)	g	working fluid vapor phase
	heat transfer coeff.	(kW/(m^{2}K))	G	working fluid phase
L	length	(m)	l	working fluid liquid phase
M	force	(Nm)	L	liquid secondary phase
v	specific volume	(m^3/kg)	su	supply
V	volume	(m^3)		
$\dot{W}$	work rate	(kW)		
x	mass fraction	(-)		
α	void fraction	(-)		
ω	angular speed	(rad/s)		

REFERENCES

Bein, T. W., & Hamilton, J. F. (1982). Computer modeling of an oil flooded single screw air compressor. In *International compressor engineering conference.* (Paper 383)

Bell, I. H., Lemort, V., Groll, E. A., Braun, J. E., & Horton, W. T. (2012). Liquid flooded compression and expansion in scroll machines - Part i: Model development. *International Journal of Refrigeration*, *35*, 1878-1889.

Bell, I. H., Wronski, J., Sylvain, Q., & Lemort. (2014). Pseudo-pure fluid thermophysial property evaluation and the open-source thermophysical property library coolprop. *Ind. Eng. Chem. Res.*, *53*, 2498-2508.

Fujiwara, M., Kasuya, K., Matsunaga, T., & Watanabe, M. (1984). Computer modeling for performance analysis of rotary screw compressor. In *International compressor engineering conference at purdue. paper 503.*

Georges, E. (2012). *Investigation of a flooded expansion organic Rankine cycle system* (Unpublished master's thesis). University of Liege.

Igobo, O., & Davies, P. (2014). Review of low-temperature vapor power cycle engines with quasi-isothermal expansion. *Energy*, *70*, 22-34.

Imran, M., Usman, M., B-S, P., & Lee, D.-H. (2016). Volumetric expanders for low grade heat and waste heat recovery applications. *Renewable and Sustainable Energy Reviews*, *57*, 1090-1109.

Ishii, M., & Hibiki, T. (2011). *Thermo-Fluid Dynamics of Two-Phase Fflow*. Springer.

Lecompte, S., Huisseune, H., van den Broek, M., Vanslambrouck, B., & De Paepe, M. (2015). Review of organic Rankine (ORC) architectures for waste heat recovery. *Renewable and Sustainable Energy Reviews*, *47*, 448-461.

Mathison, M. M., Braun, J. E., & Groll, E. A. (2013). Modeling of a novel spool compressor with multiple vapor refrigerant injection ports. *International Journal of Refrigeration*, *36*, 1982-1997.

Smith, I. K., Stosic, N., & Aldis, C. (1996). Development of a trilateral flash cycle system: Part 3: The design of high-efficiency two-phase screw expanders. *Proceedings of the Institution of Mechanical Engineers. Part A: Journal of Power and Energy*, *208(2)*, 135-144.

Stosic, N., Kovacevic, A., Hanjalic, K., & Milutinovic, L. (1988). Mathematical modelling of the oil influence upon the working cycle of screw compressors. In *International compressor engineering conference. paper 645.*

Taniguchi, H., Kudo, K., Giedt, W. H., Park, I., & Kumazawa, S. (1988). Analytical and experimental investigation of two-phase flow screw expanders for power generation. *Journal of Engineering for Gas Turbines and Power*, *110*, 628-635.

Woodland, B. J., Braun, J. E., Groll, E. A., & Horton, W. T. (2014). Methods of increasing net work output of organic Rankine cycles for low-grade waste heat recovery. In *15th international refrigeration and air conditioning conference at purdue. paper 2190.*

Woodland, B. J., Krishna, A., Groll, E. A., Braun, J. E., Horton, W. T., & Garimella, S. V. (2013). Thermodynamic comparison of organic rankine cycles employing liquid-flooded expansion or a solution circuit. *Applied Thermal Engineering*, *61*, 859-65.

Wu, J., & Jin, G. (1988). The computer simulation of oil-flooded single screw compressors. In *International compressor engineering conference.* (Paper 646)

Zhelezny, V. P., Semenyuk, Y. V., Ancherbak, S. N., Grebenkov, A. J., & Beliayeva, O. V. (2007). An experimental investigation and modelling of the solubility, density and surface tension of 1,1,1,3,3-pentafluoropropane (R-245fa)/synthetic polyolester compressor oil solutions. *Journal of Fluorine Chemistry*, *128*, 1029-1038.

Ziviani, D., Bell, I. H., De Paepe, M., & van den Broek, M. (2014). Comprehensive model of a single screw expander for ORC-systems applications. In *22th int.compressor engineering conf. at purdue.*

Ziviani, D., Bell, I. H., De Paepe, M., & van den Broek, M. (2015). Update on single-screw expander geometry model integrated into an open-source simulation tool. In *9th Int. Conf. on Compressors and their Systems, City University of London, London.*